PAPER

Electron capture by swift ions from molecules of biological interest

IOP Publishing Journal of Physics B: Atomic, Molecular and Optical Physics
J. Phys. B: At. Mol. Opt. Phys. **51** (2018) 165201 (15pp) https://doi.org/10.1088/1361-6455/aad152

Electron capture by swift ions from molecules of biological interest

M A Quinto, P R Montenegro, J M Monti, O A Fojón and R D Rivarola

Instituto de Física Rosario and Laboratorio de Colisiones Atómicas, CONICET and Universidad Nacional de Rosario, Rosario, Argentina

E-mail: quinto@ifir-conicet.gov.ar

Received 16 April 2018, revised 29 June 2018
Accepted for publication 5 July 2018
Published 19 July 2018

Abstract

Electron capture from molecular targets impacted by swift ions, H^+, He^{2+}, Li^{3+} and C^{6+}, is investigated in the framework of the quantum-mechanical continuum distorted wave-Eikonal initial state model. Biological molecules considered are nitrogen, methane, carbon monoxide, carbon dioxide and water. In particular, for water, the calculation of the corresponding cross sections plays a fundamental role for the determination of energy deposition in biological matter. A detailed analysis on the contributions coming from different molecular orbitals to total cross sections (TCS) are discriminated as well as those of capture to fundamental and excited projectile states. A good agreement with measurements is found for cases where experimental data exist. For other systems, the theoretical results here reported are useful for the prediction of the corresponding TCS.

Keywords: electron capture, ions collision, biological molecules

(Some figures may appear in colour only in the online journal)

1. Introduction

The investigation of electronic reactions involved in collisions between ions and molecules are of relevance in many areas like plasma physics, astrophysics, medical physics and radiobiology. In particular, in radiation biology, single electron capture and single electron ionization processes are the main mechanisms leading to energy loss for swift ions penetrating the living matter at medium and high impact energies. In recent years, theoretical research on these reactions was focused on biological targets, like water and DNA components, by using different perturbative quantum-mechanical [1–4] and classical models [5–10]. In particular, two of the perturbative methods, the first Born approximation with correct boundary conditions (CB1) [11] and the continuum distorted wave-Eikonal initial state (CDW-EIS) [3, 4], were used to investigate electron ionization of targets like water molecule, by impact of H^+, He^{2+}, C^{6+} and O^{8+} beams for which experimental data is available [12–15]. On the other hand however, only a few works were presented in the literature about electron capture process by ions from molecular targets in the framework of quantum-mechanical models. In fact, previous studies mainly concern electron capture from molecules interacting with protons [16]. Regarding biological targets, like water molecule and the nucleobases of the DNA, impacted by He^{2+} and C^{6+} ions, they were theoretically studied using the classical trajectory Monte Carlo [5, 6, 17, 18]. Also, a non-perturbative theory was employed to investigate electron emission in water molecule impacted by proton [19, 20] and He^+ ion [21]. In the same framework Gabás *et al* studied ionization and electron capture process for H_2O and CO molecules impacted with H^+, He^{2+} and C^{2+} [22]. In the recent work of Luna *el al* [23] the electron emission from water molecules impacted by Li^{3+} was studied both in the coupled channel TC-BGM model and experimentally, finding that the results were in good agreement with the measurements. Even more recently, Quinto *el al* [24] calculated, within quantum-mechanical models, both electron capture and ionization total cross sections (TCS) by different ions impacting on molecules of biological interest.

In the present work, we focus our research on single electron capture using the CDW-EIS approximation. Our proposal is to investigate the behavior of molecular targets as N_2, CH_4, CO, CO_2 and H_2O, interacting with H^+, He^{2+}, Li^{3+} and C^{6+} ions beams. These molecules are of biological interest since they are usually considered as the simplest components of organic structures. In a previous work the electron capture reaction from these molecular targets was investigated [16], in the case of proton impact considering

only charge exchange to the 1s state and estimating the contribution of excited states to be of the order of 20% [25]. The aim of the present work is to determine the influence of capture to excited projectile states for the four ion beams considered, and also to establish the contribution of each molecular orbital to the TCS.

2. Theory

Let us consider an incident bare nucleus of charge Z_p impinging on an atomic target with a velocity $\boldsymbol{v}$. The impact velocities involved are high enough, to consider that the vibration and rotation times of the molecule are much larger than the characteristic collision one. It is then possible to assume that the molecular nuclei remain fixed in their initial positions during the reaction. The multi-electronic collision problem, may be reduced to the analysis of a one active electron system by considering that all the other electrons (the passive ones) remain frozen in their initial orbitals during the collision and that the active electron evolves independently of them in an effective mean field of the residual target. This approximation was first formulated, with success to study electron capture for the case of atomic targets [26] and then extended to molecular targets [27]. Later on it was applied for electron ionization of atomic and molecular targets [28, 29] (see also [30, 31] for general reviews). In the independent electron model and considering that there is just one active electron, the multi-electronic Hamiltonian can be reduced to:

$$\mathrm{H}_{el} = -\frac{1}{2}\nabla^2 + V_T(\boldsymbol{x}) + V_P(\boldsymbol{s}) + V_S(\boldsymbol{R}), \qquad (1)$$

where $\boldsymbol{x}$, ($\boldsymbol{s}$) is the active electron coordinate in the target (projectile) reference frame, $V_T(\boldsymbol{x})$ is the target potential which takes into account of the interaction of the active electron with the corresponding nucleus and the passive electrons, $V_P(\boldsymbol{s}) = -Z_P/s$ is the interaction between the bare projectile and the active electron, and $V_S(\boldsymbol{R})$ is the interaction of the projectile with the target nucleus and the passive electrons. The $V_S(\boldsymbol{R})$ potential depends only on the inter-nuclear coordinate $\boldsymbol{R}$ and thus, within the straight-line version of the impact-parameter approximation gives rise to a phase factor which only affects the projectile scattering [26, 28]. Hereafter, as we are not interested on the projectile angular distribution, we will not consider this term. We perform the calculations by means of the CDW-EIS approximation that was first introduced by Crothers and McCann to study the single ionization of H by bare-ion impact [32]. The CDW-EIS approximation was proposed to improve the large overestimation of the TCS, at intermediate impact energies, obtained within the CDW model [33], which was originated by the lack of normalization of the distorted wave functions in the initial channel. Using the same argument, the CDW-EIS approximation was introduced to investigate electron capture [34]. This approximation solves the above mentioned problem, both for ionization and electron capture and exhibits, in general, a very good agreement with existing experimental data for differential and TCS. For the sake of simplicity, we present the CDW-EIS approximation in case of an atomic target, since we choose to describe the molecular orbitals by linear combinations of atomic wave functions. CDW-EIS is the first-order of a distorted wave series in which the initial and final distorted waves in case of capture are proposed as:

Table 1. Population and binding energies of the CH_4 molecular orbitals.

Molecular orbital	Population	Binding energy ε_i (a.u.)
C_{1s}	2.0 C_{1s}	−10.68
2a1	1.133 C_{2s} + 0.867 H_{1s}	−0.84
1t2	3.399 C_{2s} + 2.601 H_{1s}	−0.46

Table 2. Population and binding energies of the N_2 molecular orbitals.

Molecular orbital	Population	Binding energy ε_i (a.u.)
N_{1s}	4.0 N_{1s}	−15.06
σ_g 2s	2.0 N_{2s}	−1.37
σ_u 2s	2.0 N_{2s}	−0.68
π_u 2p	4.0 N_{2p}	−0.62
σ_g 2p	2.0 N_{2p}	−0.57

$$\chi_i^+(\boldsymbol{x}, \boldsymbol{s}, t) = \Phi_{nlm}(\boldsymbol{x}, t)\, \mathcal{L}_i^+(\boldsymbol{s}), \qquad (2)$$

$$\chi_f^-(\boldsymbol{x}, \boldsymbol{s}, t) = \Phi_{n'l'm'}(\boldsymbol{s}, t)\, \mathcal{L}_f^-(\boldsymbol{x}). \qquad (3)$$

The initial and final distorting functions are defined as:

$$\mathcal{L}_i^+(\boldsymbol{s}) = \exp[-i\nu_P\ \ln(vs + \boldsymbol{v}.\boldsymbol{s})], \qquad (4)$$

$$\mathcal{L}_f^-(\boldsymbol{x}) = N(\nu_T)^*\, {}_1F_1\,[-i\nu_T;\, 1;\, -i(vx + \boldsymbol{v}.\boldsymbol{x})]. \qquad (5)$$

In equations (2) and (3), n, m, l and n', m', l' are the quantum numbers that characterize the initial and final states respectively. Also, in equations (4) and (5), $\nu_P = Z_P/v$, and $\nu_T = \tilde{Z}_T/v$, being $\tilde{Z}_T$ an effective target charge. This charge is chosen in correspondence with the energy of each initial atomic orbital, as $\tilde{Z}_T = \sqrt{-2n^2\varepsilon_i}$, where ε_i is the corresponding electron energy. In the case of a molecular target, the ε_i electron energy is selected as the one of each one of molecular orbitals. Moreover, in (5), $N(\nu_T) = \Gamma(1 - i\nu_T)\exp(\pi\nu_T/2)$ is the normalization factor of the ${}_1F_1$ confluent hypergeometric function. Besides, the Φ_{nlm} and $\Phi_{n'l'm'}$ time-dependent wave functions corresponding to the initial and final states, are given by:

$$\Phi_{nlm}(\boldsymbol{x}, t) = \phi_i^{nlm}(\boldsymbol{x})\exp[-i\varepsilon_i t], \qquad (6)$$

$$\Phi_{n'l'm'}(\boldsymbol{x}, \boldsymbol{s}, t) = \phi_f^{n'l'm'}(\boldsymbol{s})\exp\left[-i\varepsilon_f t + i\boldsymbol{v}.\boldsymbol{x} - i\frac{1}{2}v^2 t\right], \qquad (7)$$

where $\phi_i^{nlm}(\boldsymbol{x})$ is the time independent initial bound wave function and $\phi_f^{n'l'm'}$ is the corresponding hydrogenic function with charge Z_P describing the final bound state. Also, $\varepsilon_f = -Z_P^2/(2n'^2)$ is the final projectile orbital energy.

Table 3. Population and binding energies of the CO molecular orbitals.

Molecular orbital	Population	Binding energy ε_i (a.u.)
O_{1s}	2.0 O_{1s}	−19.92
C_{1s}	2.0 C_{1s}	−10.87
1σ	1.207 O_{2s} + 0.178 O_{2p} + 1.2074 C_{2s} + 0.178 C_{2p}	−1.41
2σ	0.627 O_{2s} + 0.985 O_{2p} + 0.386 C_{2s} + 0.002 C_{2p}	−0.74
1π	2.980 O_{2p} + 1.020 C_{2p}	−0.63
3σ	0.026 O_{2s} + 0.085 O_{2p} + 0.776 C_{2s} + 1.113 C_{2p}	−0.53

Table 4. Population and binding energies of the CO_2 molecular orbitals.

Molecular orbital	Population	Binding energy ε_i (a.u.)
O_{1s}	4.0 O_{1s}	−19.87
C_{1s}	2.0 C_{1s}	−10.93
$3\sigma_g$	1.278 O_{2s} + 0.164 O_{2p} + 0.558 C_{2s}	−1.46
$2\sigma_u$	1.306 O_{2s} + 0.130 O_{2p} + 0.564 C_{2s}	−1.38
$4\sigma_g$	0.594 O_{2s} + 1.026 O_{2p} + 0.380 C_{2s}	−0.71
$3\sigma_u$	0.544 O_{2s} + 1.120 O_{2p} + 0.336 C_{2p}	−0.66
$1\pi_u$	2.492 O_{2p} + 1.508 C_{2p}	−0.65
$1\pi_g$	4.00 O_{2p}	−0.51

The *prior* version of the transition amplitude for electron capture within CDW-EIS approximation can be written as:

$$\mathscr{A}_{if}^{-}(\boldsymbol{\rho}) = -i\int_{-\infty}^{+\infty} dt\,\langle\chi_f^-|\left[\left(H_{el} - i\frac{\partial}{\partial t}\right)|\chi_i^+\rangle\right]. \tag{8}$$

By employing the Fourier transform, the $\mathscr{A}_{if}^{-}(\rho)$ can be expressed as a function of the transverse momentum transfer $\boldsymbol{\eta}$:

$$\mathcal{R}_{if}^{-}(\boldsymbol{\eta}) = \int d\boldsymbol{\rho}\exp(i\boldsymbol{\rho}.\,\boldsymbol{\eta})\mathscr{A}_{if}^{-}(\boldsymbol{\rho}). \tag{9}$$

Finally, the TCS for electron capture is obtained as:

$$\sigma_{if} = \int d\boldsymbol{\eta}\ |\mathcal{R}_{if}^{-}(\boldsymbol{\eta})|^2. \tag{10}$$

The analytic expressions of the scattering amplitude $\mathcal{R}_{if}^{-}(\boldsymbol{\eta})$ for atomic orbitals were reported by Martínez and co-workers [34]. The different final states of the projectile, characterized by the quantum numbers $n'l'm'$, are obtained by applying the derivative operator $\mathscr{D}_{n'l'm'}$ upon a generating function $\psi(\beta, \boldsymbol{\mu}, \boldsymbol{r})$, which was previously used in the case of electron excitation of hydrogenic atoms by impact of bare-ions ([35]; see also [36] for electron capture).

The description of the different initial ground state molecular orbitals are assumed to be obtained by linear combinations of their atomic compound orbitals (LCAOs). The corresponding binding energies are computed employing a self-consistent field method (MO-LCAO-SCF), whereas a complete neglected of differential overlap (CNDO) approximation is employed for the effective occupation electron analysis of the different molecular orbitals [37]. The LCAO description of the different molecular orbitals were taken out from [38] for N_2, from [39] for CH_4, from [40] for CO, from [41] for CO_2, from [37] for H_2O. Thus, the TCS involved in its LCAO description, is given by:

Table 5. Population and binding energies of the H_2O molecular orbitals.

Molecular orbital	Population	Binding energy ε_i (a.u.)
1a1	2.0 O_{1s}	−19.84
2a1	1.48 O_{2s} + 0.52 H_{1s}	−1.18
1b2	1.18 O_{2p} + 0.82 H_{1s}	−0.67
3a1	0.22 O_{2s} + 1.44 O_{2p} + 0.34 H_{1s}	−0.54
1b1	2.0 O_{2p}	−0.46

$$\sigma = \sum_{i=1}^{N}\sum_{j=1}^{N_i} c_{i,j}\sigma_{at,j} \tag{11}$$

with N the number of molecular orbitals and N_i the number of atoms that describe each molecular orbital. $\sigma_{at,j}$ refers to the atomic orbital TCS involved in its LCAO description. Besides, $c_{i,j}$ refers to the corresponding atomic effective occupation electron numbers. The different ground state atomic orbitals are describe using Roothaan–Hartree–Fock atomic wave functions [42].

In previous works, different descriptions of the molecular ground state have been used in order to analyze their influences on total and differential cross sections. For example, Galassi and co-workers have studied the electron capture process for the same molecular targets here presented, impacted by protons [16]. In that work, they used two different initial molecular descriptions: Bragg's rule and LCAO, and no significant difference in the TCS has been reported. Additionally, in 2014, Tachino *et al* investigated, among others, the influence of the description of the initial

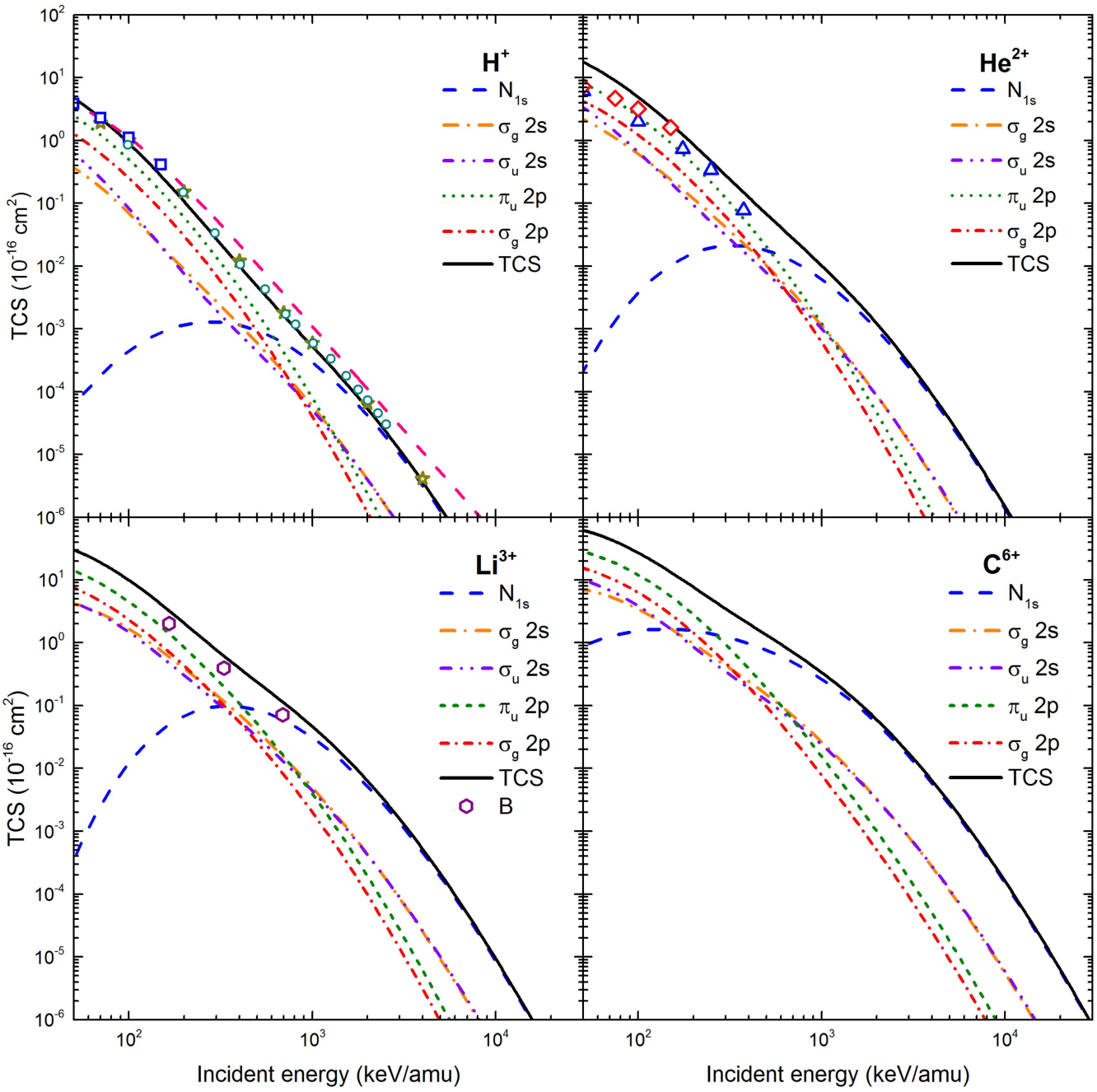

Figure 1. Cross sections calculated with CDW-EIS for single electron capture from N_2 molecule by different bare-ion impact as a function of the incident projectile energy: contribution of the initial states. Experimental data: H^+: stars Barnett *et al* [45], squares Rudd *et al* [46], circles Toburen *et al* [47], pink dashed line fitting formula Rudd *et al* [46]; He^{2+}: triangles Barnett *et al* [45], squares Rudd *et al* [48]; Li^{3+}: hexagons triangles Nokilaev *et al* [49].

target ground state, in the framework of the CDW-EIS approximation for ionization of water molecules interacting with ion beams [3]. As they have shown, only small differences are found when double differential cross sections are calculated using a CNDO or a more elaborated molecular mono-centric Moccia description of the initial ground state of water [43]. More recently, Gulyás *et al* have investigated ionization and electron capture from water molecules impacted by protons [44]. In their work, two different representations of the initial ground state of the water molecule were employed. One that takes into account the geometrical distribution of the molecule where the internuclear distance between H and O atoms was considered, and a second one corresponding to a CNDO description. They asserted that there is no influence of the two different descriptions in terms of TCS for both reactions. Supported by these results, in the present work, we have decided to use by simplicity the CNDO approximation.

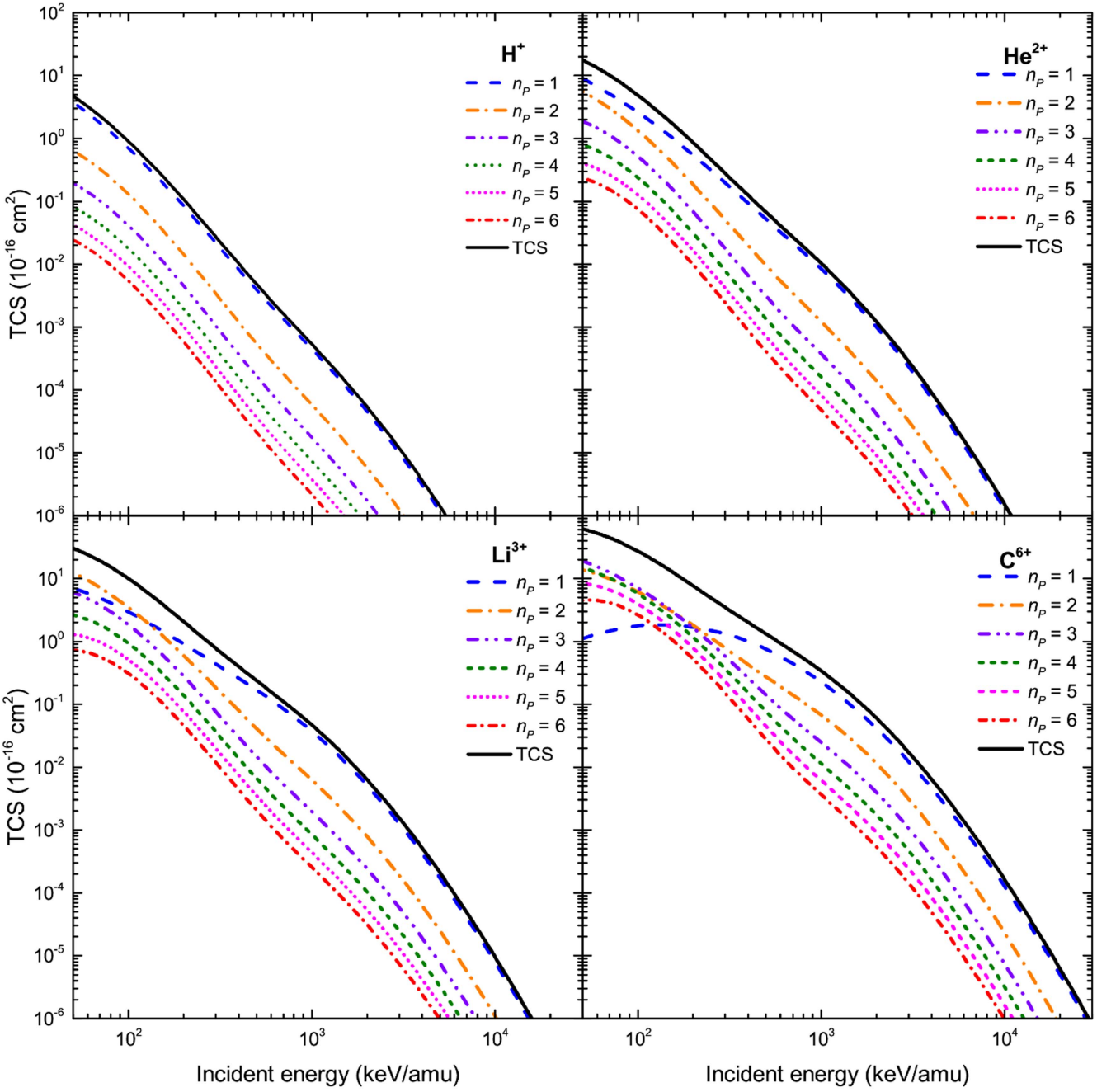

Figure 2. Cross sections calculated with CDW-EIS for single electron capture from N_2 by different bare-ion impact as a function of the incident projectile energy: contribution of the final states.

In tables 1–5 the corresponding electronic population and the binding energies for the investigated molecules are reported.

3. Results

In this section, we report the TCS for single electron capture from N_2, CH_4, CO, CO_2 and H_2O molecules impacted by ion beams, namely H^+, He^{2+}, Li^{3+} and C^{6+}, calculated within the prior version of the CDW-EIS approximation. In figures 1, 3, 5, 7 and 9, we show for each molecule the contribution to the TCS of the different molecular orbitals. And, in the figures 2, 4, 6, 8 and 10, we present, for a given molecule, the contribution of capturing to hydrogenic projectile states with principal quantum number ranging from $n = 1$ to $n = 6$.

In figure 1 the case of N_2 is analyzed. As charge exchange is a momentum transfer reaction it is well known that for atomic targets the process is preferable as the collision velocity approaches the mean velocity of the orbital electron one. Thus, for all the considered projectiles, at low-intermediate impact energies the contribution of the two outer

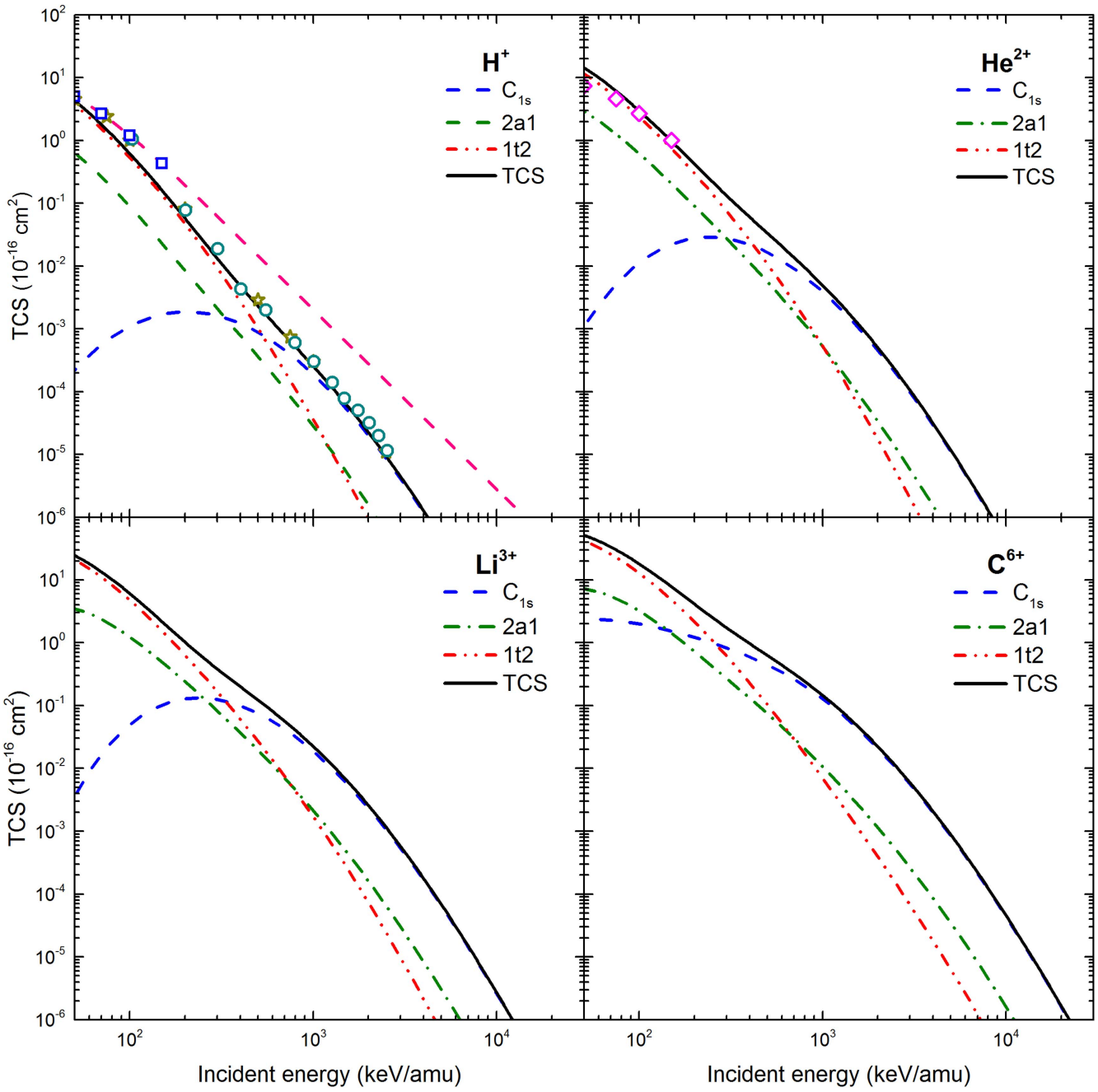

Figure 3. Cross sections calculated with CDW-EIS for single electron capture from CH_4 by different bare-ion impact as a function of the incident projectile energy: contribution of the initial states. Experimental data: H^+: stars Barnett *et al* [45], squares Rudd *et al* [46], circles Toburen *et al* [47], pink dashed line fitting formula Rudd *et al* [46]; He^{2+}: diamonds Rudd *et al* [48].

orbitals (which present comparable orbital energies) dominates the TCS. In particular, the preferable contribution from the $\pi_u 2p$ orbital must be attributed to the fact that its occupation number is 4 whereas $\sigma_g 2p$ is occupied only by two electrons. The $\sigma_g 2s$ and $\sigma_u 2s$ orbitals, which present a N_{2s} character, contribute in a similar way over all the collision energy range here considered. As the impact velocity increases the situation is reversed, dominating thus the inner orbitals. At enough high collision energies, the deepest orbital of the molecules gives the largest contribution to the TCS. This effect appears to be more noticeable as the projectile charge increases. It should be also noted that electron capture TCS from the most bound orbital presents maxima at impact velocities of the order of the orbital velocity, not depending on the projectile considered. The present theoretical cross sections are in good agreement with the existing experimental data for proton, alpha and Li^{3+} ions.

In figure 2, the contribution from all target orbitals to projectile states with different principal quantum number n is discriminated. In general, the capture to $n = 1$ dominates the TCS, decreasing the contribution as n increases. However, in the low-intermediate collision energy, namely below a few

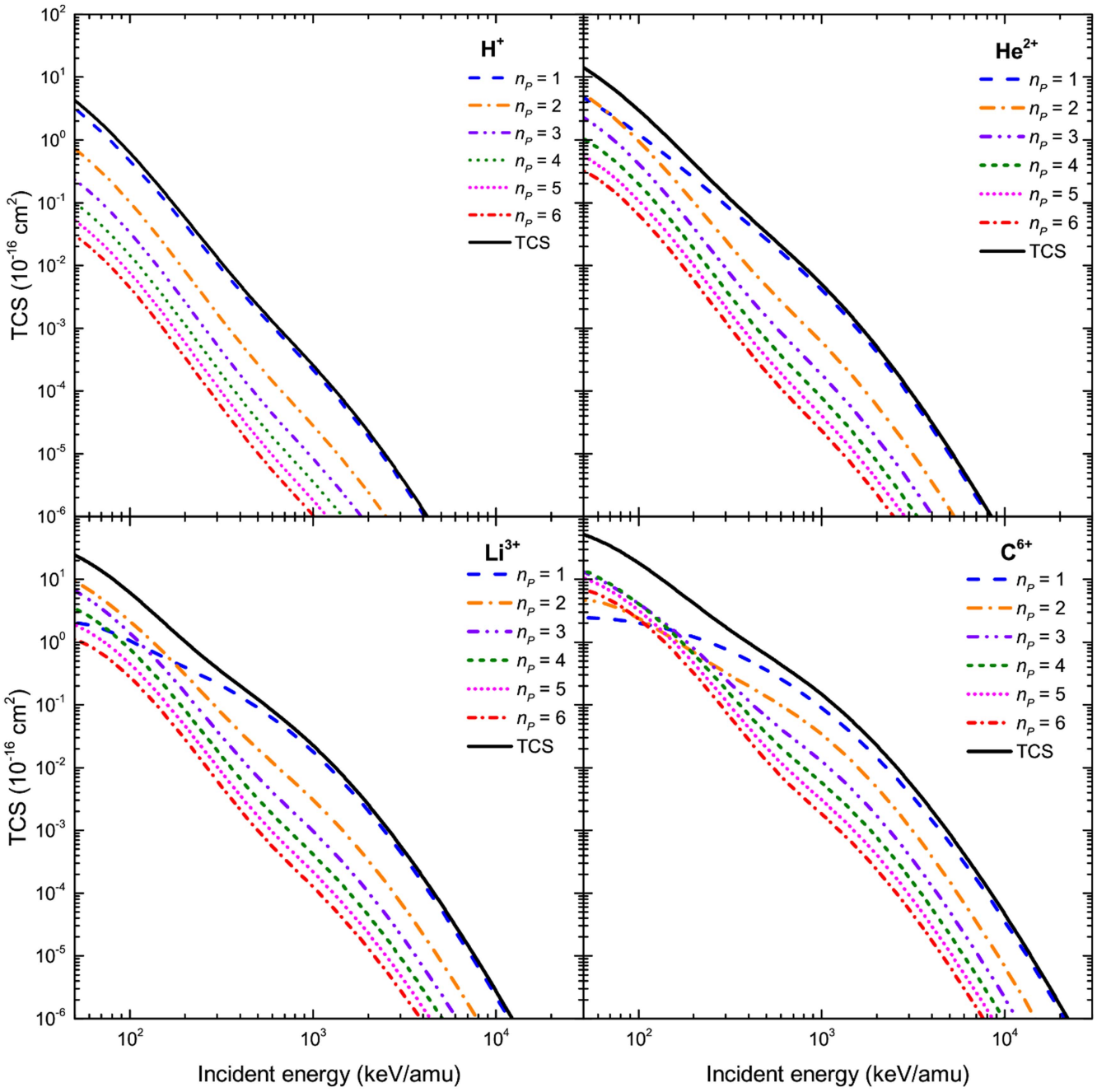

Figure 4. Cross sections calculated with CDW-EIS model for single electron capture from CH_4 by different bare-ion impact as a function of the incident projectile energy: contribution of the final states.

hundreds of keV/amu, this regular behavior is lost as the projectile charge increases, and the curve corresponding to the ground state shows a maximum, crossing the curves corresponding to outer projectile stats.

In figure 3, the case corresponding to the CH_4 molecule is presented. Having only three molecular orbitals, the effect of the dominance of TCS by less (more) bound orbitals at intermediate-low (high) impact energies is put in evidence. Again, the TCS corresponding to the most bound molecular orbital present maxima at approximately the same collision energies, independently of the projectile considered, except for the case of C^{6+} impact. A good agreement with experimental data for proton and alpha particle impact is found.

In figure 4, where the contribution of capture to TCS from all molecular orbitals to states with different principal quantum number is discriminated, a similar behavior as for the N_2 is obtained. Thus, charge exchange to the ground state dominates at high enough collision velocities for all projectiles considered, decreasing its contribution as n increases. Again, at low-intermediate energies the contribution of

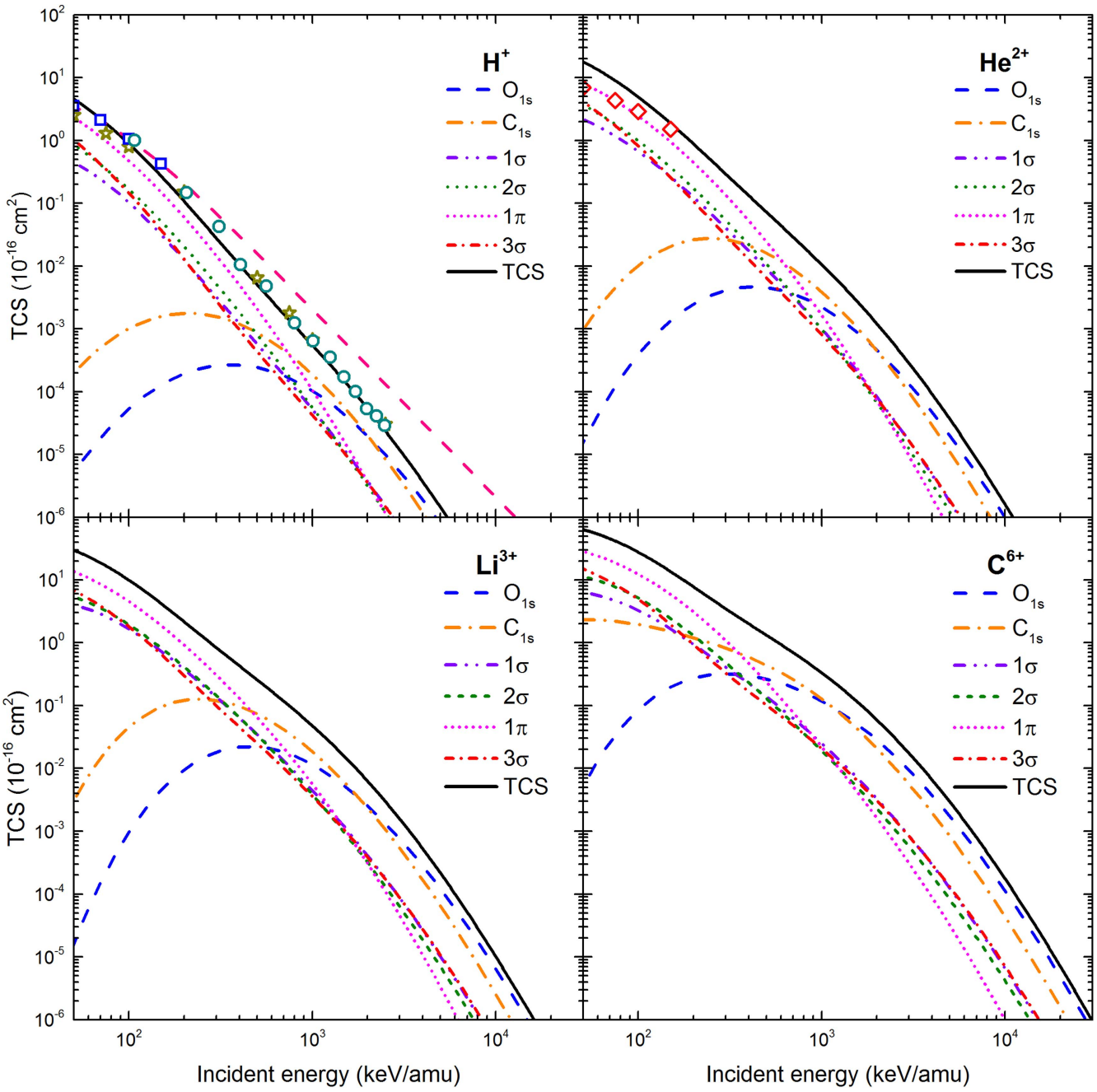

Figure 5. Cross sections calculated with CDW-EIS for single electron capture from CO by different bare-ion impact as a function of the incident projectile energy: contribution of the initial states. Experimental data: H^+: stars Barnett *et al* [45]; diamond Rudd *et al* [46], circles Toburen *et al* [47], pink dashed line fitting formula Rudd *et al* [46]; He^{2+}: squares Rudd *et al* [48].

capture to $n = 1$ strongly decreases, in such a way that TCS are dominated by the less bound electrons.

In general, the behaviors found for N_2 and CH_4 are also observed for the other three molecules investigated (see figures 5–10). In particular, for carbon monoxide and carbon dioxide (see figures 5 and 7) the two most inner orbitals (which present O_{1s} and C_{1s} atomic characters) show TCS maxima, the one corresponding to C_{1s} at lower collision energies than the one for O_{1s}, according to the electron mean velocity of these atomic states. We must note that these molecular orbitals have corresponding bound energies of the same order, which are much larger than the ones of the outer states. This is in contrast with what happens for all the other molecular targets considered, which present a mono-centric character with only one orbital much more bound than the other ones and so only one peak is found. The maxima of outer electrons, which could be expected to appear at lower impact energies, are not found in the energy range considered. For the CO and CO_2 molecules a general good agreement with measurements is obtained for proton impact. In both cases, the comparison with experimental data for alpha particles appears as difficult considering the

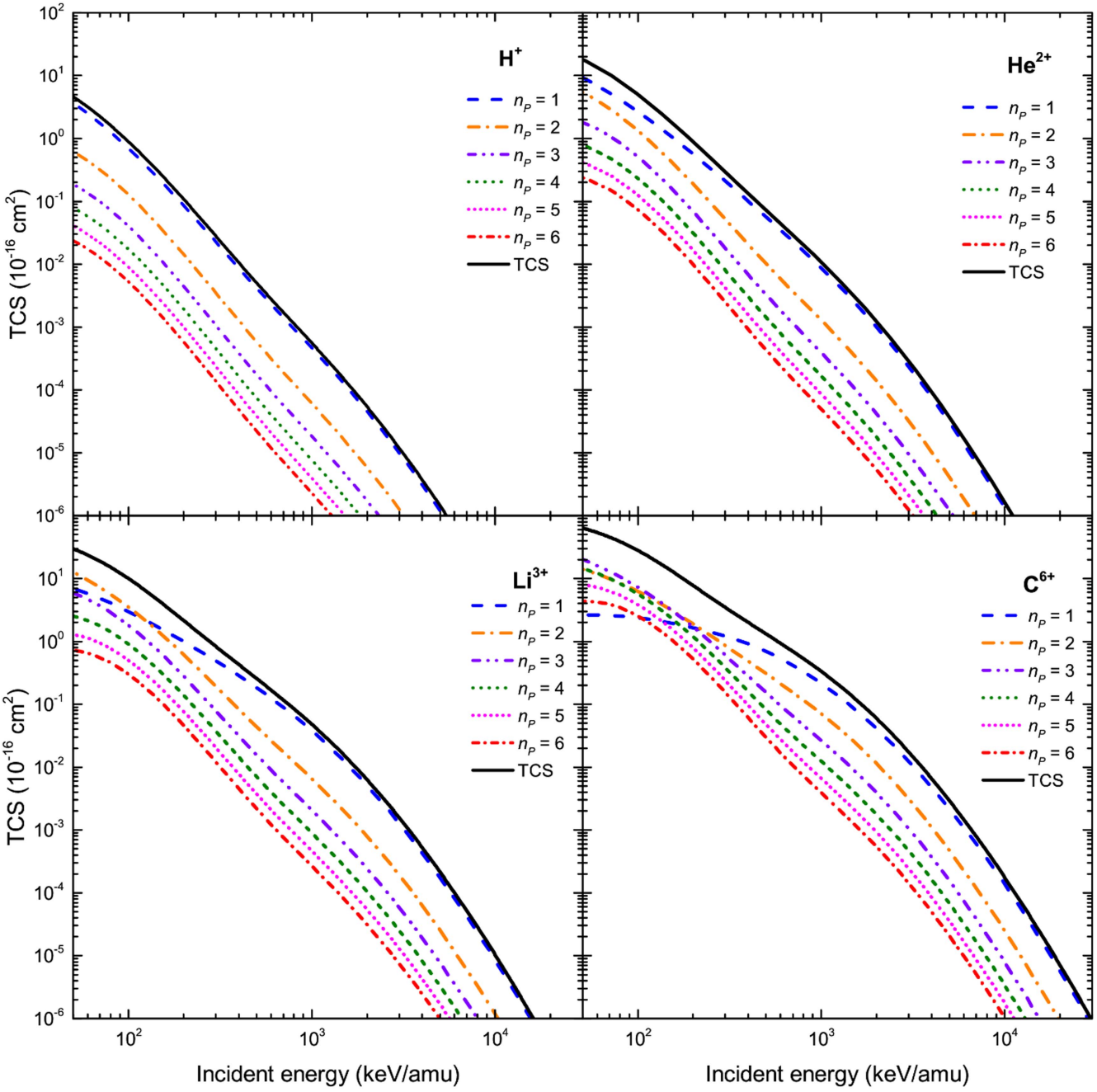

Figure 6. Cross sections calculated with CDW-EIS model for single electron capture from CO by different bare-ion impact as a function of the incident projectile energy: contribution of the final states.

scarce number of measurements, available only at low velocities. In some cases, the *n*-state partial cross sections intersect among them, resulting in a reordering of dominance of their contribution to the TCS.

For the CO molecule, the fact that the 1π orbital governs the 3σ one at enough low collision energies, being the electrons less bound for the 1π state, can be explained, as it has been done for N_2 by the occupancy number of electrons of each one of these orbitals. We can see in table 3 that the occupancy number is equal to 4 in the first case and to 2 in the second one.

We should remark that for all the five studied molecules, the present theoretical prediction exhibits a good agreement with the experimental data for the case of proton impact. A good agreement is observed for the CH_4 molecule impacted by He^{2+}, see figure 3. For the N_2 molecule, some overestimation of measurements is obtained at low-intermediate collision energies for the case of He^{2+} and Li^{3+} ions impact, see figure 1. The

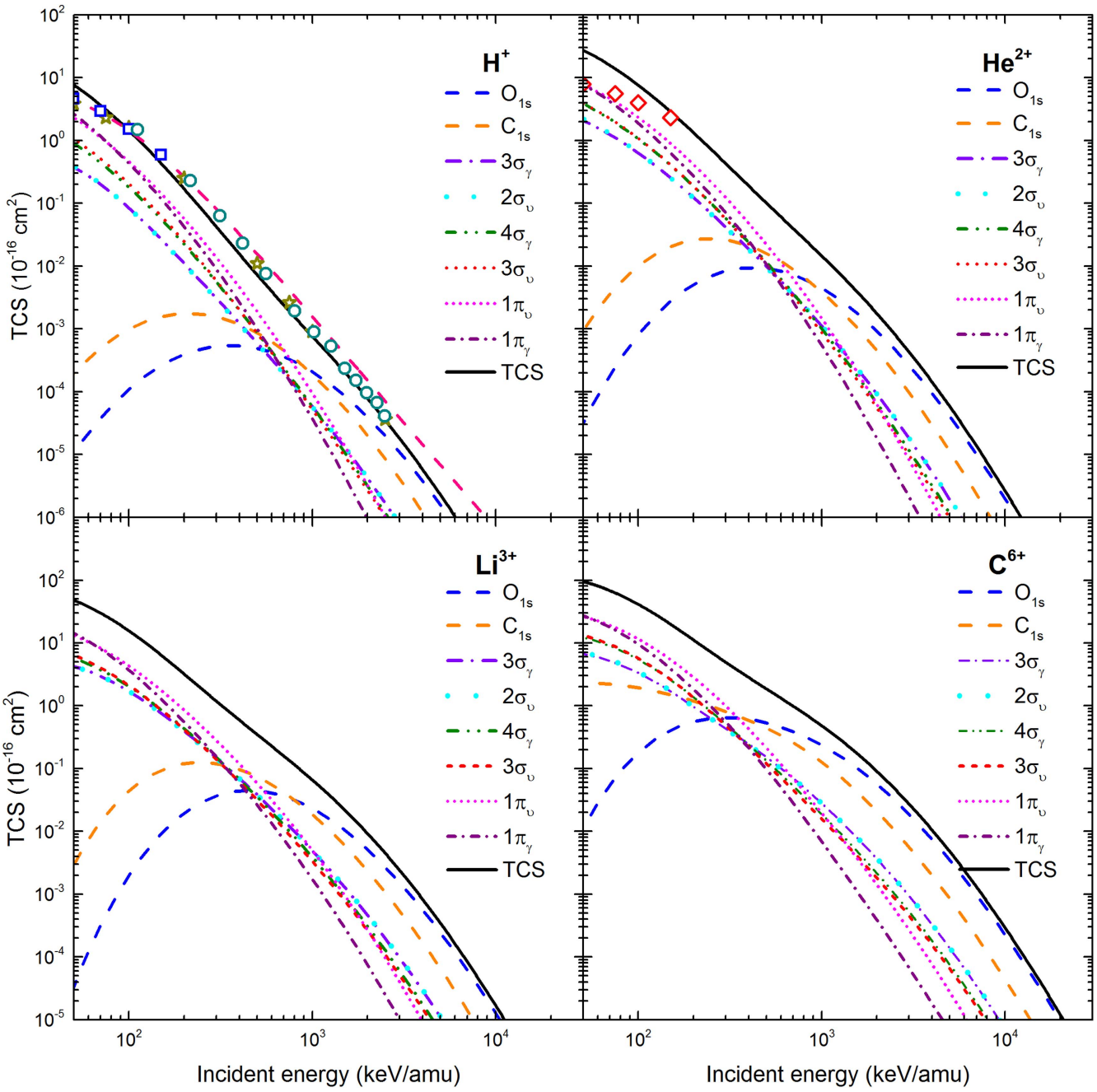

Figure 7. Cross sections calculated with CDW-EIS model for single electron capture from CO_2 by different bare-ion impact as a function of the incident projectile energy: contribution of the initial states. Experimental data, H^+: stars Barnett *et al* [45]; squares Rudd *et al* [46], circles Toburen *et al* [47], pink dashed line fitting formula Rudd *et al* [46]; He^{2+}: diamonds Rudd *et al* [48].

same discrepancy in the low energy range, namely, below 200 keV amu^{-1} is observed for the case of CO, CO_2 and H_2O molecules impacted by He^{2+}, see figures 5, 7 and 9. Whereas, for the collisional system Li^{3+} on H_2O, the theoretical results are in accordance with the experiments for energies above 200 keV amu^{-1}, see figure 9.

In figures 1, 3, 5, 7 and 9, we report a comparison with the TCS obtained with a fitting formula proposed by Rudd *et al* [46]. The analysis has been done for the case of proton projectile for the presented molecular target, except for the water molecule where the fitting formula proposed by Rudd *et al* [52] was used. In general, we observe an agreement of these results, obtained with the fitting formula, both with the experiment data and the theoretical CDW-EIS results for the incident energy less than a few hundred keV. Beyond these energies, the results overestimate both the experimental data and the present CDW-EIS calculations. Only for the case of CO_2 molecule, see figure 7, the fitting formula gives a good

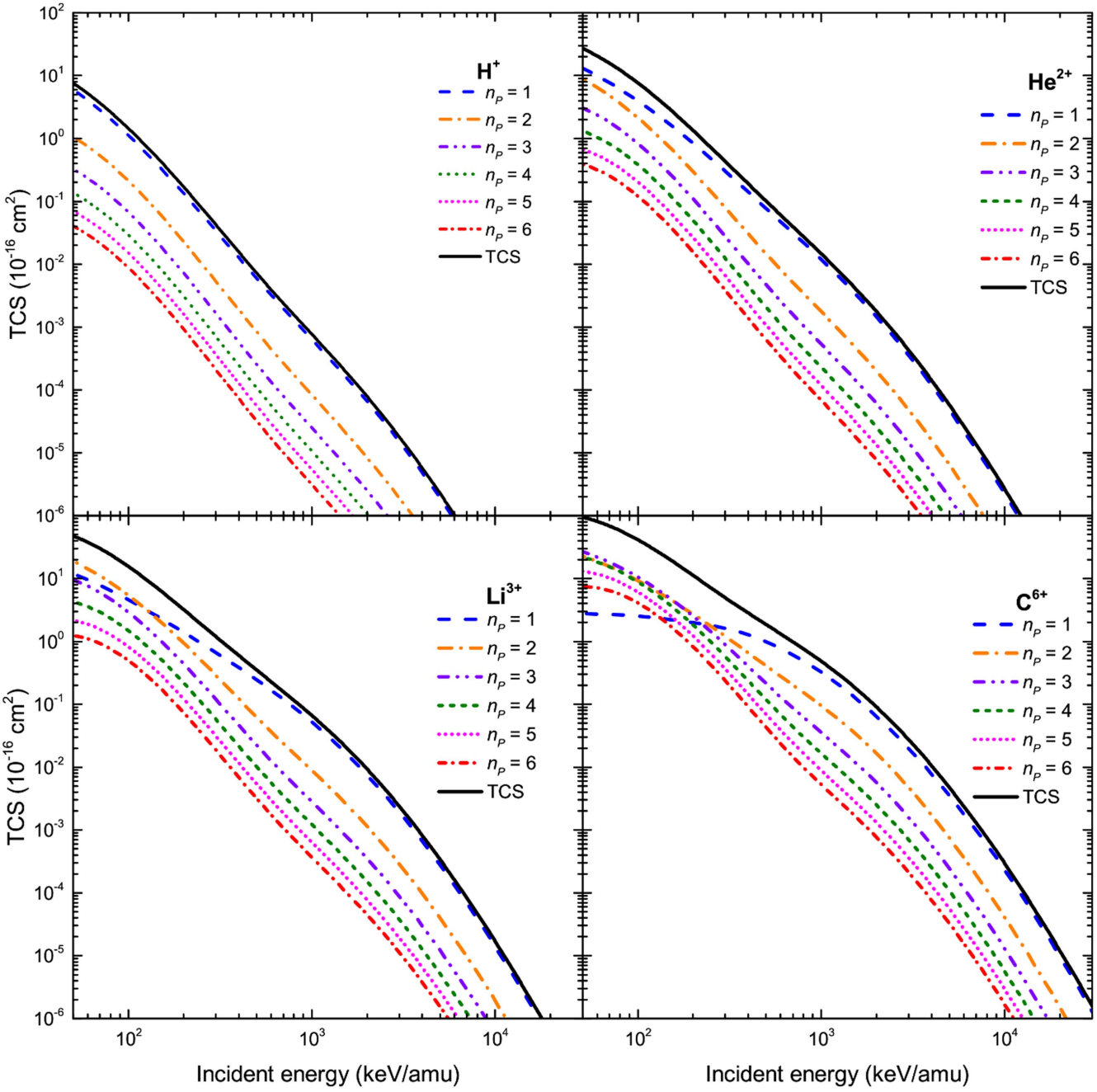

Figure 8. Cross sections calculated with CDW-EIS model for single electron capture from CO_2 by different bare-ion impact as a function of the incident projectile energy: contribution of the final states.

estimation of the TCS, which is in agreement with both experimental and present theoretical results in almost all of considered energy range. For the H_2O molecule, see figure 9, the theoretical results computed with CDW-EIS-MO approximation by Gulyás *et al* [44] was reported. In general; in the all presented energy range, the present CDW-EIS and the CDW-EIS-MO results are close to each other.

It is interesting also to analyze the cross section ratio of the capture process for a projectile of charge Z_p to determine deviations from the Z_p^5 -scaling law of B2 (second-order Born approximation) [53], valid for 1s–1s transitions at very high non-relativistic energies. We must note that at the higher energies here presented this is the dominant transition. The results presented in figure 11 are only for the water molecule target, since a similar behavior was observed for the other investigated molecules. The cross section ratio shows a strong deviation from the B2 law that increases as Z_p increases. Just for illustration, the energies considered go to very high impact ones, where relativistic effects should be taken into account. It is interesting to

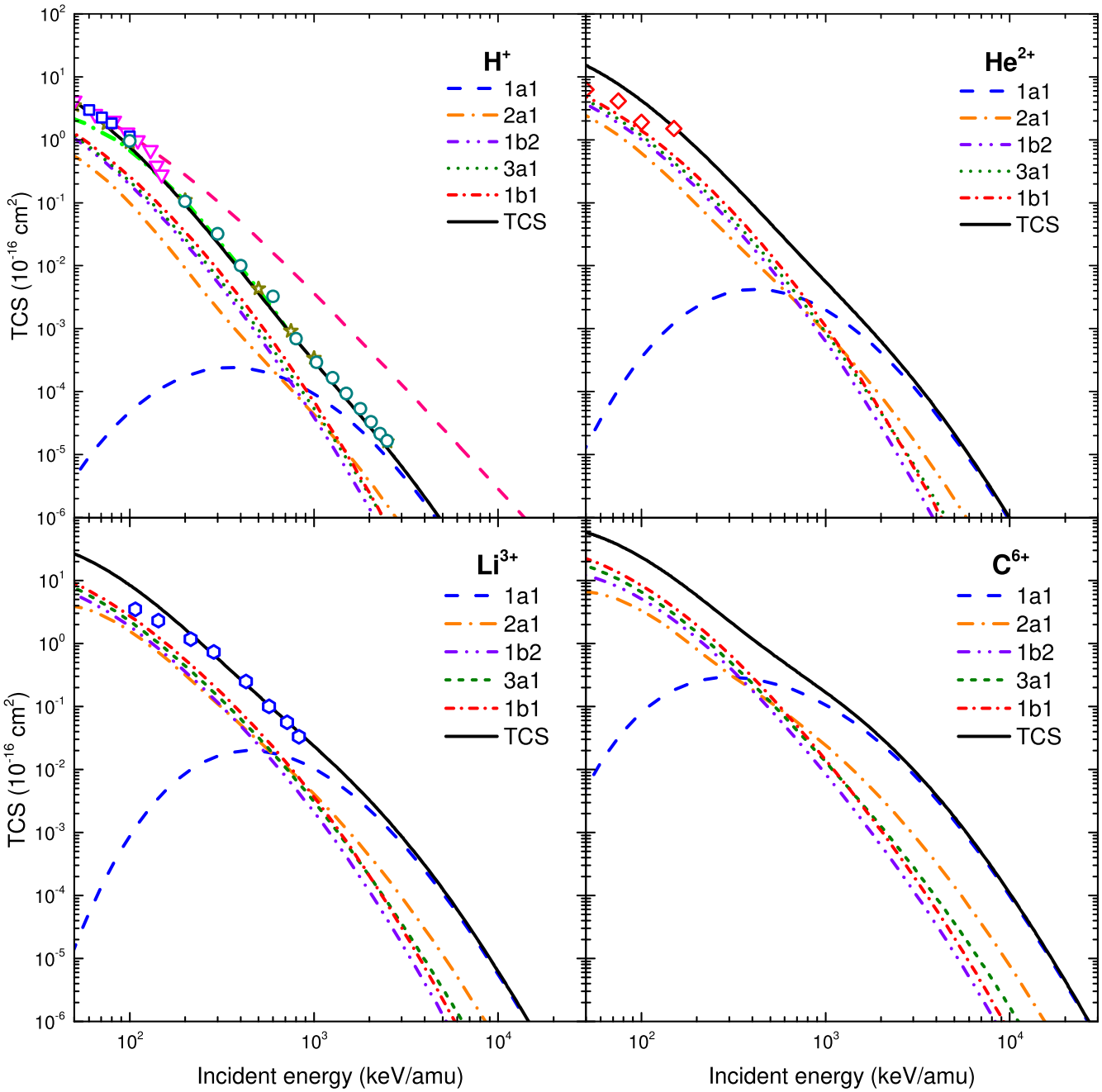

Figure 9. Cross sections calculated with CDW-EIS model for single electron capture of H_2O by different bare-ion impact as a function of the incident projectile energy: contribution of the initial states. Experimental data: H^+: stars Barnett *et al* [45], circles Toburen *et al* [47], squares Luna *et al* [50], triangles Gobet *et al* [51], pink dashed line fitting formula Rudd *et al* [52]; He^{2+}: diamonds Rudd *et al* [48]; Li^{3+}: hexagons Luna *et al* [23]. Theory H^+: CDW-EIS-MO dashed–dotted green line [44].

note that deviations are still observed at these very high energies.

Moreover, we have analyzed the cross section ratio of the capture cross sections with respect to the number of the target electrons. The results are depicted in figure 12, where only the case of He^{2+} projectile was investigated, since for the other projectiles a similar trend was observed. The TCS of each investigated molecule have been normalized by the corresponding number of electrons. As a result, all the normalized cross sections overlap one to each other in all the presented energy range. However, some negligible discrepancies are observed for the case of the CH_4 molecule. A similar result was reported for the case of both ionization and electron capture processes for water and DNA nucleobases impacted by proton [54].

4. Conclusions

In the present work, theoretical TCS for single electron capture by H^+, He^{2+}, Li^{3+} and C^{6+} ions in N_2, CH_4, CO, CO_2 and H_2O molecules are reported for impact energies ranging

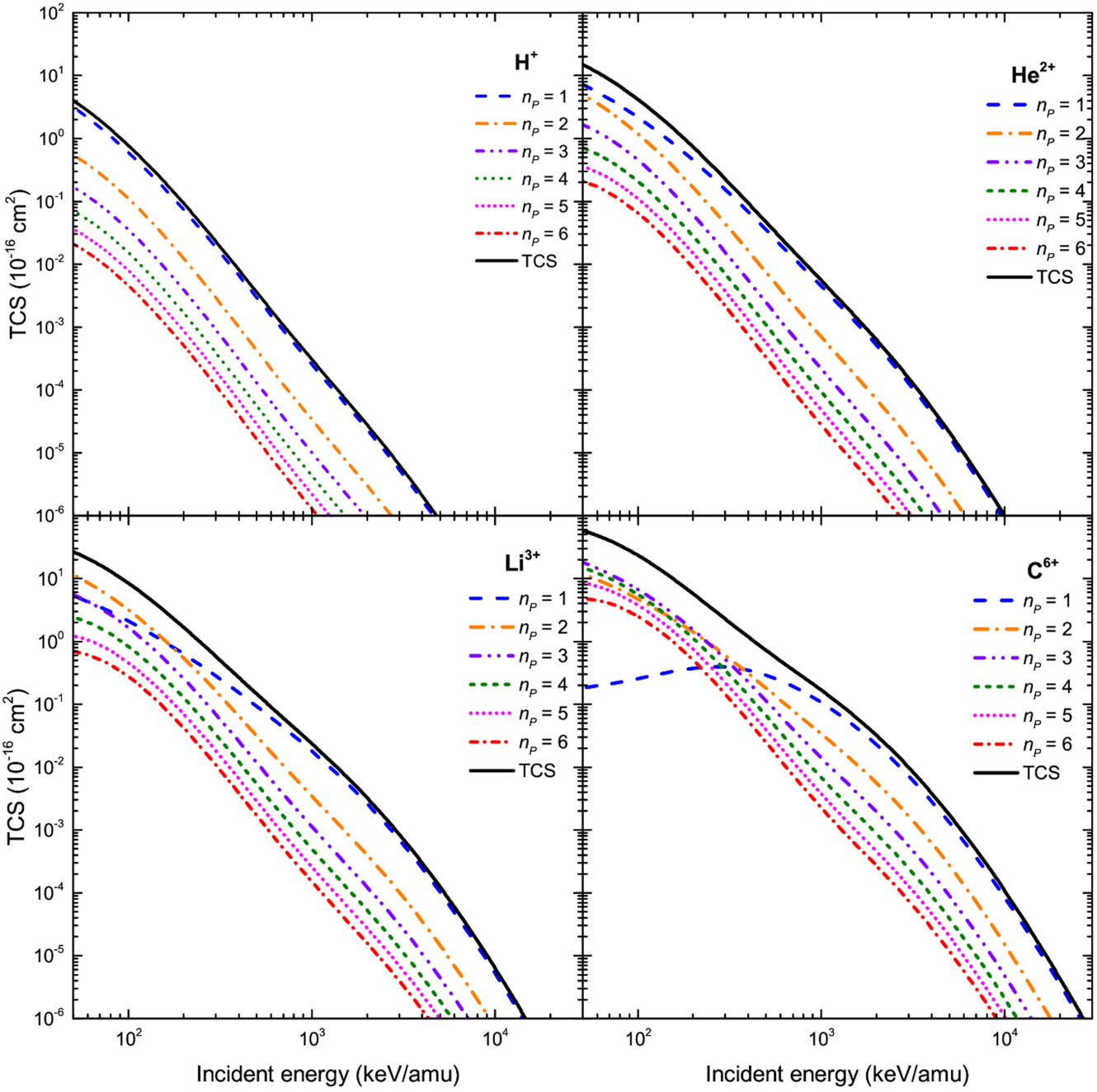

Figure 10. Cross sections calculated with CDW-EIS model for single electron capture of H_2O molecule by different bare-ions impact as a function of the incident projectiles energy: contribution of the final states.

from 50 keV amu^{-1} to 30 MeV amu^{-1}. The collisional process has been described by means of the prior version of the CDW-EIS model. The theoretical results have been compared when possible with existing experimental data. Besides, for the different collisional systems we have analyzed the influence of the higher excited state of the projectiles, from principal quantum number $n = 1$ to $n = 6$, to the TCS. It is interesting to note that the present results for molecular targets show that capture to the ground state of the projectile dominates the TCS, even for the case of multiply charged ion impact, at enough high collision velocities. It is an indication that for these energies the capture reaction is dominated by close encounters with of the nuclei of the heavier nuclear compounds. Also, the contribution of each molecular orbital to the TCS has been reported. In general, in the low-intermediate energy range, the dominant contribution to TCS is ordered from less bound to more bound orbitals. This behavior is reversed as the collision energy increases, according to minimize momentum transfer. It appears as very important the development of new experiments for which scarce data exist for the cases here analyzed. They will be useful for dosimetry codes employed in radiotherapy. It is expected that the theoretical predictions here presented could partially cover this lack of measurements.

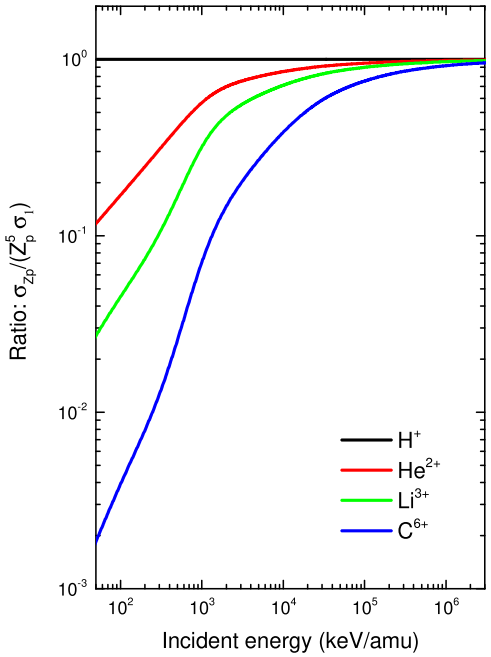

Figure 11. Cross sections ratio for the case of the water molecule target. Present CDW-EIS results solid line: black, H^+; red, He^{2+}; green, Li^{3+}; blue, C^{6+}.

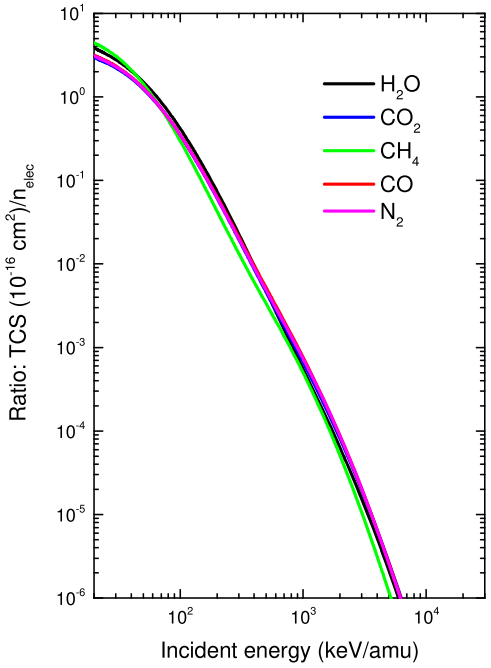

Figure 12. Cross sections ratio normalize per target electrons for the case of the He^{2+} projectile. Present CDW-EIS results solid line: black, H_2O; blue, CO_2; green, CH_4; red, CO; magenta N_2.

Acknowledgments

The authors acknowledge financial support support from the Agencia Nacional de Promoción Científica y Tecnológica through the project PICT 2015-3392 and from Consejo Nacional de Investigaciones Científicas y Técnicas through the project PIP 1026, both institutions from República Argentina.

ORCID iDs

M A Quinto https://orcid.org/0000-0002-1598-9128

References

[1] Champion C, Weck P F, Lekadir H, Galassi M E, Fojón O A, Abufager P, Rivarola R D and Hanssen J 2012 *Phys. Med. Biol.* **57** 3039
[2] Galassi M E, Champion C, Weck P F, Rivarola R D, Fojón O A and Hanssen J 2012 *Phys. Med. Biol.* **57** 2081
[3] Tachino C A, Monti J M, Fojón O A, Champion C and Rivarola R D 2014 *J. Phys. B: At. Mol. Opt. Phys.* **47** 035203
[4] Monti J M, Tachino C A, Hanssen J, Fojón O A, Galassi M E, Champion C and Rivarola R D 2014 *Appl. Radiat. Isot.* **83** 105
[5] Abbas I, Champion C, Zarour B, Lasri B and Hanssen J 2008 *Phys. Med. Biol.* **53** N41
[6] Lekadir H, Abbas I, Champion C and Hanssen J 2009 *Nucl. Instrum. Methods Phys. Res.* B **267** 1011
[7] Illescas C, Errea L F, Méndez L, Pons B, Rabadán I and Riera A 2011 *Phys. Rev.* A **83** 052704
[8] Lekadir H, Abbas I, Champion C, Fojón O A, Rivarola R D and Hanssen J 2009 *Phys. Rev.* A **79** 062710
[9] Liamsuwan T and Nikjoo H 2013 *Phys. Med. Biol.* **58** 641
[10] Nikjoo H, Emfietzoglou D, Liamsuwan T, Taleei R, Liljequist D and Uehara S 2016 *Rep. Prog. Phys.* **79** 116601
[11] Champion C, Lekadir H, Galassi M E, Fojón O A, Rivarola R D and Hanssen J 2010 *Phys. Med. Biol.* **55** 6053
[12] Ohsawa D, Tawara H, Soga F, Galassi M E and Rivarola R D 2013 *Phys. Scr.* **T156** 014039
[13] Nandi S, Biswas S, Khan A, Monti J M, Tachino C A, Rivarola R D, Misra D and Tribedi L C 2013 *Phys. Rev.* A **87** 052710
[14] Bhattacharjee S *et al* 2016 *J. Phys. B: At. Mol. Opt. Phys.* **49** 065202
[15] Bhattacharjee S, Biswas S, Monti J M, Rivarola R D and Tribedi L C 2017 *Phys. Rev.* A **96** 052707
[16] Galassi M E, Abufager P N, Fainstein P D and Rivarola R D 2010 *Phys. Rev.* A **81** 062713
[17] Dal Cappello C, Champion C, Boudrioua O, Lekadir H, Sato Y and Ohsawa D 2009 *Nucl. Instrum. Methods Phys. Res.* B **267** 781
[18] Tran H N, Dao D D, Incerti S, Bernal M A, Karamitros M, Nhan Hao T V, Dang T M and Francis Z 2016 *Nucl. Instrum. Methods Phys. Res.* B **366** 140
[19] Errea L F, Illescas C, Méndez L and Rabadán I 2013 *Phys. Rev.* A **87** 032709
[20] Murakami M, Kirchner T, Horbatsch M and Lüdde H J 2012 *Phys. Rev.* A **85** 052704
[21] Murakami M, Kirchner T, Horbatsch M and Lüdde H J 2012 *Phys. Rev.* A **86** 022719
[22] Gabás P M M, Errea L F, Mández L and Rabadán I 2012 *Phys. Rev.* A **85** 012702
[23] Luna H, Wolff W, Montenegro E C, Tavares A C, Lüdde H J, Schenk G, Horbatsch M and Kirchner T 2016 *Phys. Rev.* A **93** 052705
[24] Quinto M A, Monti J M, Montenegro P R, Fojón O A, Champion C and Rivarola R D 2017 *Eur. Phys. J.* D **71** 35
[25] Belkić D, Gayet R and Salin A 1979 *Phys. Rep.* **56** 279

[26] Rivarola R D, Piacentini R D, Salin A and Belkić D 1980 *J. Phys. B: At. Mol. Phys.* **13** 2601
[27] Corchs S E, Rivarola R D and McGuire J H 1993 *Phys. Rev.* A **47** 3937
[28] Fainstein P D, Ponce V H and Rivarola R D 1988 *J. Phys. B: At. Mol. Opt. Phys.* **21** 287
[29] Galassi M E, Rivarola R D and Fainstein P D 2004 *Phys. Rev.* A **70** 032721
[30] Fainstein P D, Ponce V H and Rivarola R D 1991 *J. Phys. B: At. Mol. Opt. Phys.* **24** 30912
[31] Stolterfoht N, DuBois R D and Rivarola R D 1997 *Electron Emission in Heavy Ion-Atom Collisions* (Berlin: Springer)
[32] Crothers D S F and McCann J F 1983 *J. Phys. B: At. Mol. Phys.* **16** 3229
[33] Belkić D 1979 *J. Phys. B: At. Mol. Phys.* **11** 3529
[34] Martínez A E, Deco G R, Rivarola R D and Fainstein P D 1988 *Nucl. Instrum. Methods Phys. Res.* B **34** 32
[35] Ramírez C A and Rivarola R D 1995 *Phys. Rev.* A **52** 4972
[36] Abufager P N, Martínez A E, Rivarola R D and Fainstein P D 2004 *J. Phys. B: At. Mol. Opt. Phys.* **37** 817
[37] Siegbahn K *et al* 1969 *ESCA Applied to Free Molecules* (Amsterdam: North-Holland)
[38] Scherr C W 1955 *J. Chem. Phys.* **23** 569
[39] Hoffmann R 1963 *J. Chem. Phys.* **39** 1397
[40] Mulliken R S 1955 *J. Chem. Phys.* **23** 1833
[41] Allan C J, Gelius U, Allison D A, Johansson G, Siegbahn H and Siegbahn K 1972 *J. Electron Spectrosc. Relat. Phenom.* **1** 131
[42] Clementi E and Roetti C 1974 *At. Data Nucl. Data Tables* **14** 177
[43] Moccia R 1964 *J. Phys. Chem.* **40** 2186
[44] Gulyás L, Egri S, Ghavaminia H and Igarashi A 2016 *Phys. Rev.* A **93** 032704
[45] Barnett C, Ray J A, Ricci E, Wilker M I, McDaniel E W, Thomas E W and Gilbody H B 1977 *Atomic Data for Controlled Fusion Research* (Springfield, VA: Oak Ridge National Laboratory)
[46] Rudd M E, DuBois R D, Toburen L H, Ratcliffe C A and Goffe T V 1983 *Phys. Rev.* A **28** 3244
[47] Toburen L H, Nakai M Y and Langley R A 1968 *Phys. Rev.* **171** 114
[48] Rudd M E, Goffe T V and Itoh A 1985 *Phys. Rev.* A **32** 2128
[49] Nikolaev V S, Dmitriev I S, Fateeva L N and Teplova Y A 1961 *Sov. Phys.-JETP* **13** 695
[50] Luna H *et al* 2007 *Phys. Rev.* A **75** 042711
[51] Gobet F *et al* 2004 *Phys. Rev.* A **70** 062716
[52] Rudd M E, Goffe T V, DuBois R D and Toburen L H 1985 *Phys. Rev.* A **31** 492
[53] Briggs J S and Dubé L 1980 *J. Phys. B: At. Mol. Phys.* **13** 771
[54] Champion C, Quinto M A, Monti J M, Galassi M E, Weck P F, Fojón O A, Hanssen J and Rivarola R D 2015 *Phys. Med. Biol.* **60** 7805–28